Tissue Eng Regen Med (2022) 19(3):629–642
https://doi.org/10.1007/s13770-022-00437-5

Online ISSN 2212-5469

ORIGINAL ARTICLE

Thermosensitive Hydrogel Loaded with Primary Chondrocyte-Derived Exosomes Promotes Cartilage Repair by Regulating Macrophage Polarization in Osteoarthritis

Xuehan Sang[1] · Xiuhong Zhao[2] · Lianqi Yan[3] · Xing Jin[1] · Xin Wang[1] · Jianjian Wang[1] · Zhenglu Yin[1] · Yuxin Zhang[4] · Zhaoxiang Meng[1]

Received: 27 December 2021 / Revised: 19 January 2022 / Accepted: 24 January 2022 / Published online: 18 April 2022

Abstract

BACKGROUND: Intra-articular injection is a classic strategy for the treatment of early osteoarthritis (OA). However, the local delivery of traditional therapeutic agents has limited benefits for alleviating OA. Exosomes, an important type of extracellular nanovesicle, show great potential for suppressing cartilage destruction in OA to replace drugs and stem cell-based administration.

METHODS: In this study, we developed a thermosensitive, injectable hydrogel by in situ crosslinking of Pluronic F-127 and hyaluronic acid, which can be used as a slow-release carrier to durably retain primary chondrocyte-derived exosomes at damaged cartilage sites to effectively magnify their reparative effect.

RESULTS: It was found that the hydrogel can sustainedly release exosomes, positively regulate chondrocytes on the proliferation, migration and differentiation, as well as efficiently induce polarization of M1 to M2 macrophages. Intra-articular injection of this exosomes-incorporated hydrogel significantly prevented cartilage destruction by promoting cartilage matrix formation. This strategy also displayed a regenerative immune phenotype characterized by a higher infiltration of $CD163^+$ regenerative M2 macrophages over $CD86^+$ M1 macrophages in synovial and chondral tissue, with a concomitant reduction in pro-inflammatory cytokines (TNF-α, IL-1β, and IL-6) and increase in anti-inflammatory cytokine (IL-10) in synovial fluid.

CONCLUSION: Our results demonstrated that local sustained-release primary chondrocyte-derived exosomes may relieve OA by promoting the phenotypic transformation of macrophages from M1 to M2, which suggesting a great potential for the application in OA.

Keywords Primary chondrocyte-derived exosomes · Hydrogel · Osteoarthritis · Cartilage repair · Macrophage polarization

Xuehan Sang and Xiuhong Zhao contribute equally to this work.

✉ Yuxin Zhang
yuxinzhang0129@163.com

✉ Zhaoxiang Meng
yzmzx001@163.com

[1] Department of Rehabilitation, Northern Jiangsu People's Hospital, Yangzhou 225001, China

[2] Department of Integrated Traditional Chinese and Western Medicine, People's Hospital of Qinghai Provincial, Xining 810007, China

[3] Department of Orthopedics, Northern Jiangsu People's Hospital, Yangzhou 225001, China

[4] Department of Rehabilitation Medicine, Shanghai Ninth People's Hospital, Shanghai Jiao Tong University School of Medicine, Shanghai 200011, China

1 Introduction

Osteoarthritis (OA) is a highly prevalent type of chronic joint disease characterized by cartilage destruction, synovial inflammation, osteophyte formation and remodeling of subchondral bone, that affects over 300 million people worldwide [1]. Chronic pain and motion dysfunction caused by OA seriously impair the life quality of sufferers and increase the economic burden. Articular cartilage is an avascular tissue with limited self-healing capability. Therefore, articular cartilage degeneration is usually regarded as an irreversible pathological change [2]. Joint replacement is regarded as the preferred candidate for end-stage OA, but patients have to bear the economic burden and long recovery time, as well as some unbearable post-operative complications (e.g., prosthesis loosening and periprosthetic infection) which result the failure of implantation [3, 4]. Therefore, it is of great significance to develop early non-surgical treatment to alleviate the progression of OA.

Over the past few decades, the transplantation of chondrocytes and mesenchymal stem cells (MSCs) have received a huge amount of attention and arisen as very promising candidates for preventing articular cartilage destruction in OA [5–8]. However, MSCs often exhibit undesirable in cell phenotype, proliferation and differentiation capabilities when cultured *in vitro* after multiple passages or extracted from aged and/or diseased donors [9]. In addition, after intra-articular administration, only a few cells adhere to the cartilage defects, their differentiation ability is not well controlled and prominent in the joint cavity [10, 11]. Undesired hypertrophy and ossification of newly formed tissue can also be observed in stem cell-based cartilage regeneration [12, 13]. Recently, there is growing evidence that, compared with direct differentiation into target tissues, transplanted stem cells are more likely to function in the articular cavity through paracrine mode, especially by secreting extracellular vesicles [13, 14]. As the most prominent extracellular vesicles, exosomes (usually 30–150 nm in diameter) can be secreted by various cells and mediate intercellular communication via their contents, including various types of lipids, nucleic acids, and proteins. Exosomes are considered important mediators of cell–cell communication and cellular immunity that participate in multifarious physiological and pathological processes [15–17]. Exosomes have similar functions as the derived cells, such as MSCs-derived exosomes exhibit a beneficial therapeutic effect on OA [18, 19]. Moreover, studies have demonstrated that primary chondrocyte-derived exosomes had enviable bioactivity in eliminating mitochondrial dysfunction and restoring immune regulation, as well as promoted articular cartilage repair [20, 21]. However, few studies have detected the therapeutic effect and the underlying mechanism of action for exosomes derived from primary chondrocytes in OA.

Furthermore, cartilage regeneration usually takes a relatively long period of time, and it is difficult to durably retain exosomes at the damaged cartilage sites to exert their continuous chondroprotective effect in OA by direct intra-articular injection. Hydrogels, three-dimensional (3D) network composed of hydrophilic polymers, have been adopted as carriers for the controlled release of various elements (e.g., cells, drugs, and bioactive molecules) for tissue regeneration, owing to their unique features (such as biocompatibility, high water content, swelling behavior, modulated 3D networks and high matrix mimetics) [22–26]. In this study, a thermosensitive, injectable hydrogel was prepared by in situ crosslinking of Pluronic F-127 and hyaluronic acid for encapsulation and sustained release of primary chondrocyte-derived exosomes. To research the potential mechanism of preventing cartilage destruction in OA, we investigated the effects of exosomes encapsulated in hydrogel on chondrocytes proliferation, survival, migration, and matrix synthesis, as well as macrophages polarization and associated cytokines secretion (Fig. 1).

2 Materials and methods

2.1 Isolation and characterization of primary chondrocyte-derived exosomes

Articular cartilage was dissected from the femoral condyles and tibial plateaus of sprague–dawley (SD) rat on postnatal day 5–6, as described previously [27]. Chondrocytes were maintained as a monolayer in Dulbecco's modified eagle's

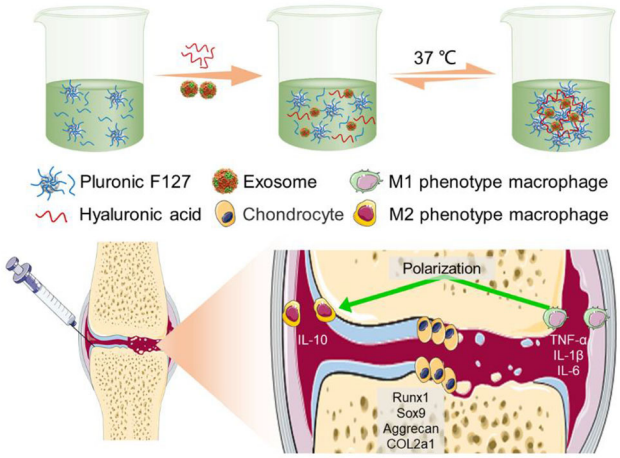

Fig. 1 Schematic illustration of exosomes-incorporated F127-HA hydrogel for inducing efficient polarization of M1 to M2 macrophages and cartilage protection in OA

medium (DMEM, Gibco, Grand Island, NY, USA) supplemented with 10% fetal bovine serum (FBS, Gibco) and 1% streptomycin–penicillin solution (Gibco) at 37 °C. The exosomes were isolated and extracted according to the classical differential centrifugation method [28].

Briefly, when chondrocytes attained 70–80% confluency, they were washed twice with PBS and cultured in serum-free medium for 48 h. The medium was centrifuged at 300 *g* for 10 min and 2000 *g* for 10 min at 4 °C. Subsequently, the supernatant was collected and filtered by a 0.22 μm filter (Merck Millipore, Billerica, MA, USA) to remove cell debris. The supernatant was then transferred to an Amicon Ultra-15 centrifugal filter (Burlington, VT, USA) and centrifuged at 4000 *g* at 4 °C until the volume was reduced to 200 μL. For exosome purification, the medium was placed on a 30% sucrose/D_2O cushion in an Ultra-Clear™ tube (Beckman Coulter, CA, USA). Then, the liquid was centrifuged at 100,000 *g* for 60 min at 4 °C to remove microvesicles. The obtained pellets were resuspended and centrifuged at 4000 *g*, and stored at −80 °C or used immediately for the experiment.

The morphology of exosomes was observed by a transmission electron microscopy (TEM). The concentration and size distribution of exosomes were evaluated by Nanoparticle Tracking Analyzer (NTA) (v3.1, Malvern Instruments, Ltd., Worcestershire, UK). The presence of exosome surface marker proteins, including CD63, CD9, and CD81were analyzed by western blotting. Cellular uptake of exosomes was studied by labelling the exosomes with Dil solution (Eugene, OR, USA).

2.2 Hydrogel preparation and characterization

A simple mixing process was used to develop the Pluronic F-127 (Sigma, St. Louis, MO, USA) and hyaluronic acid (Bioland, Cheonan, Korea) (F127-HA) hydrogel in aqueous solution according to previous studies [29, 30]. Briefly, Pluronic F-127 (20 wt%) and HA (1 wt%) were dissolved in deionized water at 4 °C to obtain a transparent solution. Then, exosomes (10 mg) were added into F127-HA solution (10 ml) and mixed well by gently stirring, and stored at 4 °C for subsequent experiments.

The F127-HA solution was subsequently warmed to 37 °C to realize the sol–gel transition. To determine the critical gelation temperature of sol–gel transition, rheological measurement was performed from 0 to 40 °C by a rheometer (Malvern, UK). The morphology of the F127-HA hydrogel was observed by a field emission scanning electron microscopy (FE-SEM) (JSM-7000F, JEOL, Tokyo, Japan) at 3 kV after freeze-drying. To investigate the degradation behavior, hydrogel samples were placed in PBS (pH 7.4) at 37 °C for fully swelling and the initial weight (W_0) of the samples were weighed. At pre-determined intervals, the hydrogels were taken out and their weights (W_t) were recorded. The remaining weight (%) of F127-HA hydrogels was calculated by the following equation: remaining weight (%) = $(W_0-W_t)/W_0 \times 100$. To examine the release profiles, 1 ml exosomes-incorporated hydrogel was immersed in 2 mL PBS and incubated at 37 °C. At pre-determined time points, PBS was collected and an equal amount of fresh PBS was added. The cumulative release of exosomes was evaluated with a BCA protein assay kit (Beyotime, Shanghai, China).

2.3 Cell proliferation, viability, and migration

Chondrocytes were seeded at a density of 2×10^4/well in 24-well plates and treated with 200 μl PBS (Con group), hydrogel (Gel group), exosomes (Exo group), and exosomes-incorporated hydrogel (Exo@Gel group), respectively. At 1, 4, and 7 days, cell proliferation was detected by Cell Counting Kit-8 (CCK-8) assay (Beyotime). Briefly, at the scheduled time points, 10% CCK-8 solution was added into the samples and the absorbance was evaluated by a microplate reader at 450 nm. To investigate the cell viability, dead/live staining of the samples was performed by Calcein-AM/PI kit (Beyotime) after 3 days of incubation according to the product manual. In brief, Calcein-AM and PI were added into the samples and incubated in the dark for 15 min at 4 °C. The fluorescent images were observed and photographed by fluorescence microscope (Carl Zeiss, Oberkochen, Germany), and the cell survival rate analyzed by Image J software (National Institutes of Health, Bethesda, MD, USA) according to the proportion of live cell. The migration of chondrocytes in response to different treatments was studied by Transwell test. Briefly, 5×10^4 cells were seeded in the upper chamber, and 200 μl PBS or therapeutic agents were added to the lower chambers. After 24 h, the upper surfaces of the transwell filters were swabbed free of cells. Cells on the underside of the filter were fixed by 4% (v/v) paraformaldehyde (Solarbio, Beijing, China) and stained with crystal violet (Yuanye, Shanghai, China). The cells in five randomly-selected fields were counted under a microscope.

2.4 Real-time quantitative PCR (RT-qPCR)

The gene expression of *Runx1*, *Sox 9*, *Aggrecan*, and *COL2a1* in the chondrocytes was investigated by RT-qPCR. Simply put, total RNA was extracted with TRIzol reagent (Invitrogen, Carlsbad, CA, USA), and cDNA was synthesized in reverse transcription reaction by 1 ug total RNA using a Prime Script RT reagent kit (Takara, Dalian, China). The samples were amplified by CFX Connect™ realtime PCR system (Bio-Rad, Hercules, CA, USA) with iTaq™ Universal SYBR® Green Supermix (Bio-Rad), and

primers, as shown in Table 1. Glyceraldehyde 3-phosphate dehydrogenase (*GAPDH*) was used as internal controls for relative mRNA expression. The relative mRNA expression was calculated by the $2^{-\Delta\Delta Ct}$ method, and finally expressed as fold changes.

3 Results and Discussion

3.1 Macrophage polarization and inflammatory cytokines secretion

The macrophage RAW264.7 cell line was purchased from the American Type Culture Collection (ATCC) and cultured in high glucose-DMEM containing 10% FBS and 1% streptomycin-penicillin. The RAW264.7 cells cultured in the medium were defined as M0 macrophages. The cells were stimulated by 50 ng/ml lipopolysaccharide (LPS) (Beyotime) and treated with different agents for 24 h. The samples were washed with PBS and fixed in 4% paraformaldehyde for 15 min, permeabilized with 0.2% Triton X-100 for 20 min, and blocked with PBS containing 3% BSA for 1 h. Then, cells were incubated overnight with the primary antibodies, anti-CD86 antibody (1:250, Abcam, Cambridge, UK) and anti-CD163 antibody (1:200, Abcam). Alexa 488 dye-labeled secondary antibodies (Jackson ImmunoResearch Inc., West Grove, PA, USA) were added and incubated for 1 h at room temperature. Nuclear staining was performed for 5 min by the addition of 4′,6-diamidino-2-phenylindole (DAPI) solution (Beyotime). Immunoreactivity was visualized using a fluorescence microscope. Furthermore, flow cytometry was used to further quantify the amount of M1/M2 polarization. Briefly, the cells were harvested and washed twice with FACS buffer and spined at 200 × *g* for 5 min, and then stained with approximately 50 μL cocktail of fluorochrome-conjugated antibodies including CD86 and CD163 in combination with viability dye Zombie-UV for 30 min at 4 °C (refrigerator) in the dark. After fixation and washing, the samples were transferred to a new 1 ml microcentrifuge tube for flow cytometry. In addition, the supernatant was collected and the expression levels of pro-inflammatory cytokines including tumor necrosis factor (TNF)-α, interleukin (IL)-1β, and IL-6, as well as anti-inflammatory cytokines including IL-10, were measured by enzyme linked immunosorbent assay (ELISA) kits (R&D systems, Minneapolis, MN, USA) according to the manufacturer's instructions.

Table 1 Primer sequences of genes

mRNA	Oligonucleotide Primers (5′–3′)
GAPDH	F-ATGGGAAGCTGGTCATCAAC
	R-GGATGCAGGGATGATGTTCT
Runx1	F-CTCTCAGCGGAACTTTCCAGTC′
	R-TGACAGGAGGCGAGTAGGTGAA
Sox 9	F-AGGAAGCTGGCAGACCAGTA
	R-CGGCAGGTATTGGTCAAACT
Aggrecan	F-TGGCATTGAGGACAGCGAAG
	R-TCCAGTGTGTAGCGTGTGGAAATAG
COL2a1	F-CGAGGTGACAAAGGAGAAGC
	R-CTGGTTGTTCAGCGACTTGA

3.2 OA model establishment and intra-articular injection

Healthy adult male SD rats (8-week-old) were provided by the Experimental Animal Center of Northern Jiangsu People's Hospital. All experimental protocols were conducted in accordance with the guidelines and approved by the Animal Care and Use Ethics Committee of the Northern Jiangsu People's Hospital (IACUC no. 20170312001). The surgical destabilization of the medial meniscus (DMM) OA model was prepared by the modified Hulth technique [15]. Under general anesthesia by intraperitoneal injection of 3% sodium pentobarbital (0.2 ml/100 g), the anterior cruciate ligament was cut and the medial meniscus was removed of the right knee joint. Subsequently, the incision was sutured layer by layer and penicillin was injected intramuscularly for three consecutive days. All rats undergoing DMM surgery or sham surgery were randomly divided into 5 groups (n = 10 in each group). At 4 weeks post-operation, sham operated rats without subsequent treatment were regarded as healthy group, and the OA rats were injected intra-articularly with 200 μl PBS (PBS group), hydrogel, exosomes, and exosomes-loaded hydrogel, respectively, once every 2 weeks for 3 times. The synovial fluid extracted with syringe for inflammatory cytokines detection by ELISA kits. At 12 weeks after intra-articular injection, the rats were euthanized by overdose of sodium pentobarbital and the right knee joints and synovial tissues were collected for further investigation.

3.3 Histological evaluation

The knee joint samples were fixed by 4% paraformaldehyde, decalcified in 0.5 M EDTA solution, and then embedded for paraffin. Subsequently, the sections with a thickness of 5 μm including the articular cartilage were obtained. The slices were stained with hematoxylin eosin (H&E) and safranin O-fast green (Thermo Fisher Scientific, Shanghai, China) according to the manufacturer's standard protocols. The Osteoarthritis Research Society International (OARSI) cartilage histopathology assessment system was used to evaluate the cartilage degeneration

[31]. Synovial tissues were stained with H&E dye to evaluate synovial inflammation.

3.4 Immunofluorescence

Sections of articular cartilage and synovial tissue were prepared as previously described. After dewaxing and rehydration, the slices were soaked in citrate buffer at 60 °C overnight to reveal the antigen. For immunofluorescence, the sections were incubated overnight with following primary antibody: anti-F4/80 antibody (1:200, eBioscience, USA), anti-CD86 antibody (1:250, Abcam, USA), anti-CD163 antibody (1:200, Abcam, USA), anti-Runx1 (1:300, Abcam, USA), anti-Sox 9 (1:200, Abcam, USA), anti-Aggrecan antibody (1:400, Abcam, USA), anti-COL-2a1 (1:200, Abcam, USA) at 4 °C, and then incubated with Alexa 488 or Cy3 dye-labeled secondary antibody for 1 h. Nuclei were stained with DAPI and the images were observed by a fluorescence microscope.

3.4.1 Statistical analyses

Statistical analysis was conducted by SPSS version 22.0 (SPSS Inc., Chicago, IL, USA). Statistical significance was analyzed by the Student's *t*-test, or one-way or two-way ANOVA with Tukey's post hoc test. A $p < 0.05$ was considered significant. All experiments repeated independently at least three times, and the results were presented as mean ± standard deviation.

3.4.2 Characterization of primary chondrocyte-derived exosomes

Vesicles were isolated from the supernatant of primary chondrocytes by ultrafiltration and centrifugation, and identified by TEM, NTA, and western blotting. TEM images exhibited that primary chondrocyte derived-exosomes showed a typical hollow, spherical-like morphology (Fig. 2A). NTA detection showed that the particle concentration of original exosomes-suspension was 8.14×10^{13}/ml, and the diameter of exosomes was 40–140 nm, with an average value of ~ 90 nm (Fig. 2B). In addition, western blotting analysis displayed the exosome markers CD63, CD9, and CD81were significantly enriched in exosome groups (Fig. 2C). Generally, these results revealed the successful isolation of exosomes from the supernatant of primary chondrocytes. We also investigated whether chondrocytes could acquire exosomes. Primary chondrocytes were first labeled with red fluorescent dye (Dil solution) before exosomes isolation. The chondrocytes were then treated with Dil-labeled exosomes for 6 h. Fluorescence microscopy observation indicated that Dil-labeled exosomes were located in the cytoplasm to confirm cellular uptake of exosomes (Fig. 2D).

3.4.3 F127-HA hydrogel preparation and exosomes loading

As shown in Fig. 3A, increasing the temperature from 4 to 37 °C, the F127-HA solution underwent a sol–gel transition. When the temperature was dropped to 4 °C, the hydrogel formed sol again. The reversible thermo-responsive property of the F127-HA hydrogel allows it to undergo gelation at body temperature and remain at the implantation site as a sustained drug delivery system. In addition, this attractive reversible thermo-responsive nature also endows the hydrogel with injectable property. As exhibited in Fig. 3B, the F127-HA solution can quickly form a gel after being extruded through a syringe onto the 37 °C hot plate. SEM observation indicated that the hydrogel had an interconnected pore morphology (Fig. 3C). To confirm the critical gelation temperature of sol–gel transition, the rheological behavior revealed that both the storage modulus (G') and loss modulus (G'') of the hydrogel were rapidly promoted after 21 °C, indicating that the critical gelation temperature of the F127-HA hydrogel was about 21 °C (Fig. 3D).

As a biocompatible polymer, Pluronic F-127 is widely used as a thermosensitive material due to its rapid thermo-reversible sol–gel transition and the ability to deliver drugs [30, 32]. The surfactant function of Pluronic F-127 is beneficial to the dispersion of drugs in the hydrogels, but

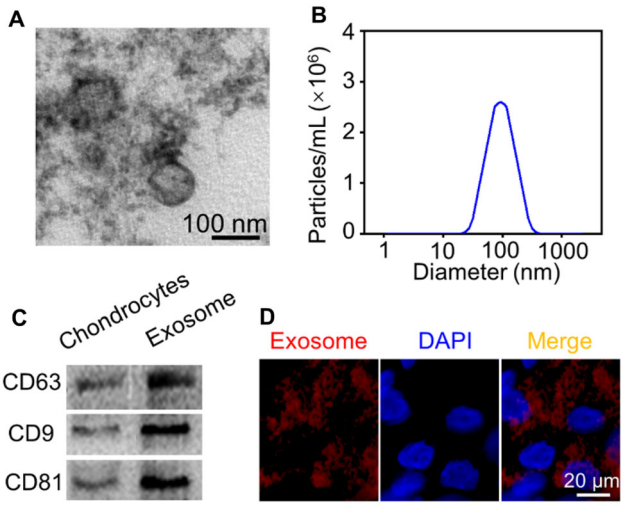

Fig. 2 Characterization and uptake of primary chondrocyte derived-exosomes. **A** TEM images exhibited the morphology of primary chondrocyte derived-exosomes. **B** NTA detection showed the particle size distribution of exosomes. **C** Western blotting evaluated the expression of exosome surface markers, CD63, CD81, and CD9. **D** Representative immunofluorescence images of Dil-labeled exosomes absorbed by chondrocytes

this performance may lead to the rapid erosion in several hours at physiological conditions, thus resulting in a rapid degradation of hydrogels and burst release of loaded-drugs [33, 34]. To address these limitations, HA, a natural biopolymer existing in synovial fluid, was incorporated into our formula. Intra-articular injection of HA, a visco-supplementation, is considered as a cost-effective strategy to prolong the pathological progression of OA [35, 36]. The addition of high-molecular-weight HA could help the dense packing of Pluronic F-127 micelles at the gelation temperature. Driving force for this phenomenon could be a hydrophobic interaction between acetyl groups on HA and methyl groups on Pluronic F-127. As a result, the inter-micellar crosslinking induced by HA may heighten the mechanical strength and retention time of the prepared thermosensitive hydrogel [29]. The F127-HA hydrogel can be completely degraded within 14 days (Fig. 3E). With the degradation of hydrogel, the cargoes were released slowly. As illustrated in Fig. 3F, the release curves indicated that the exosomes could be released continuously from hydrogel for 14 days. The curves in the first day was slightly faster, and the release rate gradually decreased in the subsequent days. Initially, exosomes diffusion likely plays a major role as the hydrogel has not yet been significantly degraded. A slightly fast release of exosomes during the initial phase may be related to absorption of the exosomes on the surface of hydrogel by electrostatic interaction. In the subsequent release period, the degradation of hydrogel likely becomes the dominant factor mediated release. The slow degradation of hydrogel enables exosomes to be released continuously and in a controlled manner [32]. This sustained-release strategy allows the exosomes to remain in the damaged cartilage site durably to exert their sustained chondroprotective effect.

3.4.4 Exo@Gel effects on chondrocytes proliferation, migration, and matrix synthesis

As the articular cartilage repair and regeneration was characterized by chondrocytes proliferation, migration, and matrix synthesis, we investigated the regulation of these processes by our exosome-loaded hydrogel. As illustrated in Fig. 4A, whether in Exo group or Exo@Gel group, the introduction of exosomes significantly enhanced cell proliferation, compared with the Con group and Gel group ($p < 0.05$). It is worth mentioning that on the 7th day, the proliferation rate of chondrocytes in the Exo@Gel group was higher than that in the Exo group ($p < 0.05$). Fluorescence images of Calcein-AM/PI staining showed that cells in each group were almost green-stained live cells (Fig. 4B). The cell survival rates of chondrocytes were about 95% after different treatments (Fig. 4C). As shown in Fig. 4D–E, we also observed that the chondrocytes incubated with exosome-loaded hydrogel showed enhanced migration ability than that of Con ($p < 0.01$), Gen group ($p < 0.01$), and Exo group ($p < 0.05$), respectively. Thus, we speculate that exosome-loaded hydrogel has the potential to induce chondrocytes proliferation and migrate to the damaged region rapidly during the repair process.

In addition to proliferation and migration, inducing matrix synthesis is a crucial issue for the management of OA. Chondrocytes synthesize sufficient matrix will contribute to the efficient repair of articular cartilage in OA. Herein, the results of RT-qPCR revealed that the expression of chondrogenic genes, including *Runx1*, *Sox9*, *Aggrecan*, and *COL2a1*, were up-regulated in the exosome treatment groups, which were significantly higher than that of Con group and Gel Group (Fig. 4F–I). Moreover, the expression of these cartilage markers in the Exo@Gel group was higher than that in the Exo group ($p < 0.05$).

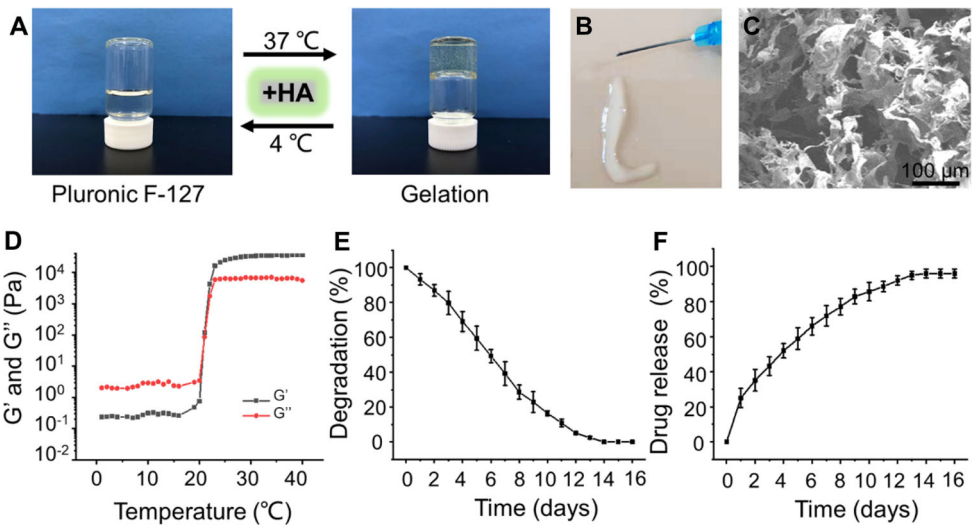

Fig. 3 Preparation and characterization of F127-HA hydrogels. **A** The optical images of hydrogel sol–gel transition. **B** Morphology of hydrogel observed by SEM. **C** The injectable and thermosensitive hydrogel rapidly form gel when injected into the hot plate at 37 °C. **D** Storage modulus (G') and loss modulus (G'') of hydrogel as a function of temperature. **E** Degradation rate of the F127-HA hydrogels in PBS at 37 °C. **F** Release profile of exosomes from the F127-HA hydrogels in PBS at 37 °C

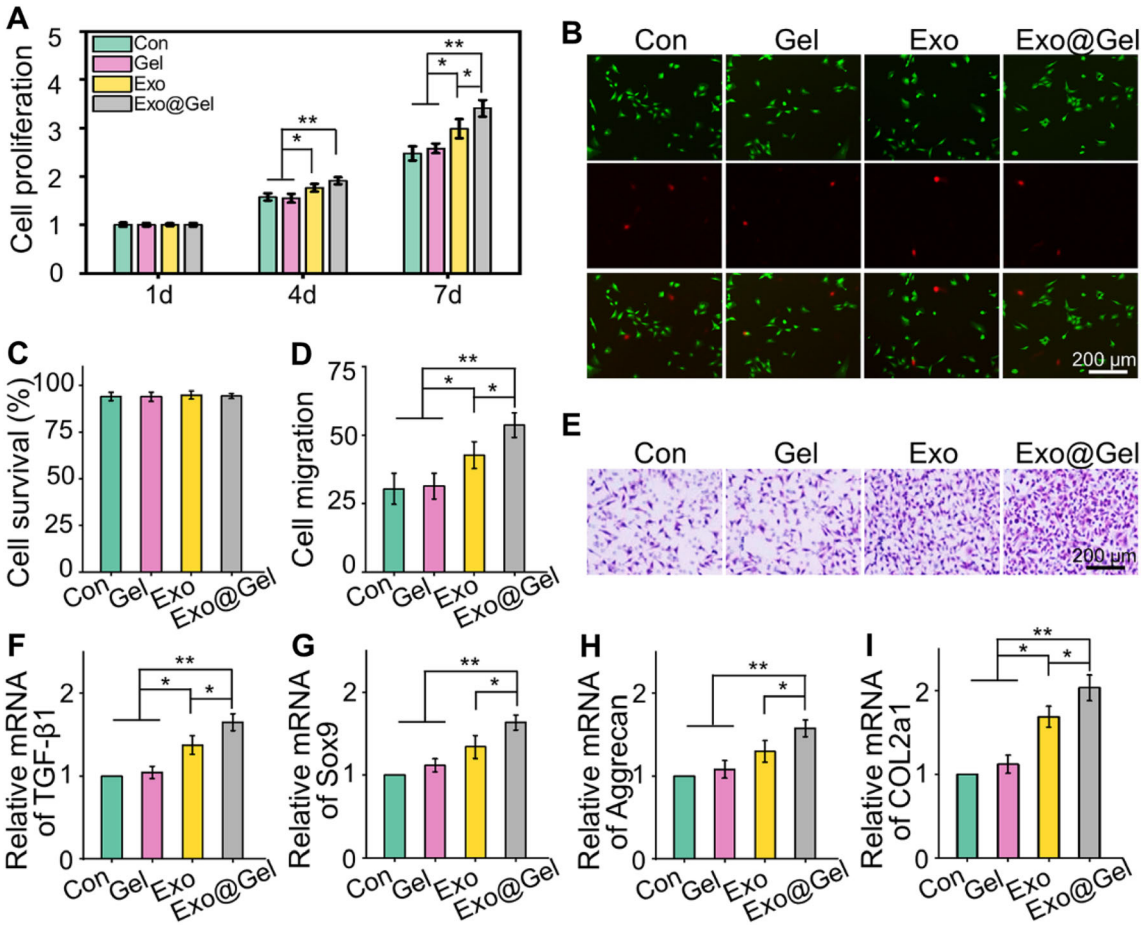

Fig. 4 Exosomes-incorporated F127-HA hydrogels promote chondrocytes proliferation, migration and differentiation. **A** Chondrocytes proliferation at day 1, 4 and 7. **B**, **C** Calcein AM/PI staining and survival rates of chondrocytes at day 3. The green signal represents live cells, whereas the red signal represents dead cells. **D**, **E** Transwell test and quantitative analysis of cell migration. **F–I** RT-qPCR analysis of chondrogenic-related genes *Runx1*, *Sox9*, *Aggrecan*, and *COL2a1* in chondrocytes after chondrogenic induction for 14 days (*$p < 0.05$, **$p < 0.01$)

Runx1 contributes to articular cartilage maintenance by enhancement of cartilage matrix production and suppression of hypertrophic differentiation [37]. Sox9 is an early chondrogenic marker, controls both chondrocytes proliferation and differentiation, which can promote the synthesis of collagen II and aggrecan [38, 39]. Previous researches have demonstrated that exosome can promote proliferation, migration, and up-regulate the expression of cartilage-specific markers (*e.g.*, Sox9, COL2a1, and Aggrecan), as well as enhance the matrix production [40–42]. Herein, our results exhibited that primary chondrocyte-derived exosomes notably induced chondrocytes proliferation and migration, up-regulated the expression of cartilage-specific genes. In addition, our results lead to an interesting conclusion that encapsulating the exosomes into F127-HA hydrogel to obtain a stable release rhythm can amplify the beneficial effect of exosomes. According to the above results, we consider that incorporating the exosomes into the hydrogel is a better candidate to as a stimulator for chondrocytes proliferation, migration, and matrix synthesis.

3.4.5 Exo@Gel promotes the phenotypic transformation of macrophages from M1 to M2 in vitro

Recently, exosomes and biomaterials have attracted considerable attention for promoting tissue repair and regeneration owing to they directly affect the immunomodulation of macrophages [43]. In the innate immune response, macrophages can be divided into two polarization states, namely classically activated M1 phenotype and alternatively activated M2 phenotype [44]. After tissue injury or being stimulated by LPS and interferon-γ, M1 macrophages secrete a large number of pro-inflammatory cytokines, such as TNF-α, IL-1β, and IL-6, to trigger the body's inflammatory response and remove dead cells. However, excessive inflammation can cause damage and continuous consumption to normal tissues

[45, 46]. In later stages of tissue repair, M2 macrophages secreting anti-inflammatory cytokines (such as IL-10, IL-4, and TGF-β) gradually increase, which can inhibit the aggravated inflammation [15]. In addition, the polarization of macrophages from the M1 to M2 phenotype has been shown to promote effective angiogenesis and tissue repair [47, 48].

We further investigated the regulation of macrophage polarization by primary chondrocyte-derived exosomes *in vitro*. LPS (50 ng/mL) was applied to induce RAW264.7 polarization to the M1 phenotype. Immunofluorescence staining of CD86 (M1 macrophages marker) and CD163 (M2 macrophages marker), as well as flow cytometry were performed to identify macrophage phenotypes, and ELISA was used to determine the content of inflammatory cytokines in the supernatant. Immunofluorescence images exhibited that the proportion of $CD86^+$ M1 macrophages was significantly up-regulated after LPS treatment. The increase of M1 polarization cannot be inhibited by hydrogel alone, but it can be counteracted by introducing exosomes, especially incorporating the exosomes into hydrogel (Fig. 5A, B). LPS treatment did not increase the proportion of M2 macrophages ($CD163^+$), but exosomes treatment significantly induced the polarization of macrophage M1 to M2 (Fig. 5C, D). Especially, the Exo@Gel group significantly inhibited the M1 polarization caused by LPS treatment without difference with the Con group, and induced M2 polarization with a higher efficiency than the Exo group ($p < 0.05$). Furthermore, flow cytometry was conducted to further quantify the amount of M1/M2 polarization. As shown in Fig. 5E, the proportions of M1 macrophages were 15.3, 76.6, 74.2, 24.3, and 22.4%, and M2 macrophages were 11.4, 9.6, 8.5, 31.9, and 36.3%, in the Con, LPS, LPS-Gel, LPS-Exo, and LPS-Exo@Gel groups, respectively. These results indicated that the Exo@Gel group significantly induced the macrophage polarization from M1 to M2 phenotype. The ELISA results demonstrated that the contents of the pro-inflammatory cytokines, including TNF-α, IL-1β, and IL-6, were significantly decreased, while the anti-inflammatory cytokine IL-10 was increased in the exosomes-treatment group, especially in the Exo@Gel group (Fig. 5F–I). These results indicated that primary chondrocyte-derived exosomes promoted the phenotypic transformation of macrophages from M1 to M2 *in vitro* and reduce inflammation. Moreover, the application of incorporating exosomes into hydrogel for stable release will result in a better induction of macrophage polarization and anti-inflammatory effects.

3.4.6 Intra-articular injection of Exo@Gel promote cartilage repair in OA

OA is a chronic joint disease, characterized synovial inflammation, articular cartilage degeneration, osteophyte formation, and joint dysfunction, which is one of the main reasons for physical disability of the elderly. In this study, we developed an early non-surgical treatment of OA by preparing an exosomes-encapsulated F127-HA hydrogel for intra-articular injection. At the 12th week after injection, as displayed in Fig. 6A, the PBS group showed severe cartilage degradation, obviously thinned articular cartilage, increased surface fibrosis region, and abnormal distribution of chondrocytes. Although the histological morphology of articular cartilage in the Gel group and Exo group remained relatively intact, the cartilage layer was thinned and the arrangement of deep chondrocytes on the articular surface was irregular and loose. However, the articular cartilage was generally intact and chondrocytes were arranged regularly in the Exo@Gel group. Moreover, Safranin O-fast green staining was carried out to observe the cartilage matrix. Exosomes-treated groups reduced the loss of cartilage matrix in OA, especially the Exo@Gel group indicating a sufficient and uniform matrix distribution (Fig. 6B). The OARSI cartilage histopathology assessment system was applied to evaluate the cartilage destruction. Specifically, the OARSI scores in the Health, PBS, Gel, Exo, and Exo@Gel groups were 2.8 ± 1.3, 13.8 ± 1.9, 11.6 ± 1.1, 7.8 ± 1.1, and 5.6 ± 1.5 (Fig. 6C), respectively, suggesting intra-articular injection of exosomes-incorporated F127-HA hydrogels can significantly prevent cartilage degeneration in OA.

To further research the expression of cartilage-related marks, immunofluorescence staining was conducted to analyze the content of Runx1, Sox 9, Aggrecan, and COL2a1 in the articular cartilage at 12 weeks post-injection (Fig. 6D). By means of quantitative analysis of the fluorescence intensity, Exo@Gel group displayed significantly higher expression of cartilage-related marks than those of in the PBS group, Gel group, and Exo group ($p < 0.05$, Fig. 6E–H). These findings indicated that primary chondrocyte-derived exosomes inhibit cartilage degradation and promote matrix synthesis during OA progression in rats, but the combination strategy of exosomes encapsulated in the hydrogel can better prevent arthritic cartilage degeneration. Previous studies have demonstrated that exosomes can prevent cartilage destruction in OA. The main mechanisms involved may be that exosomes increase extracellular matrix synthesis, suppress cartilage degradation, enhance cartilage-specific markers expression of chondrocytes, and promote directly chondrogenesis of BMSCs [42, 49, 50]. However, the degeneration and repair of articular cartilage in OA is a

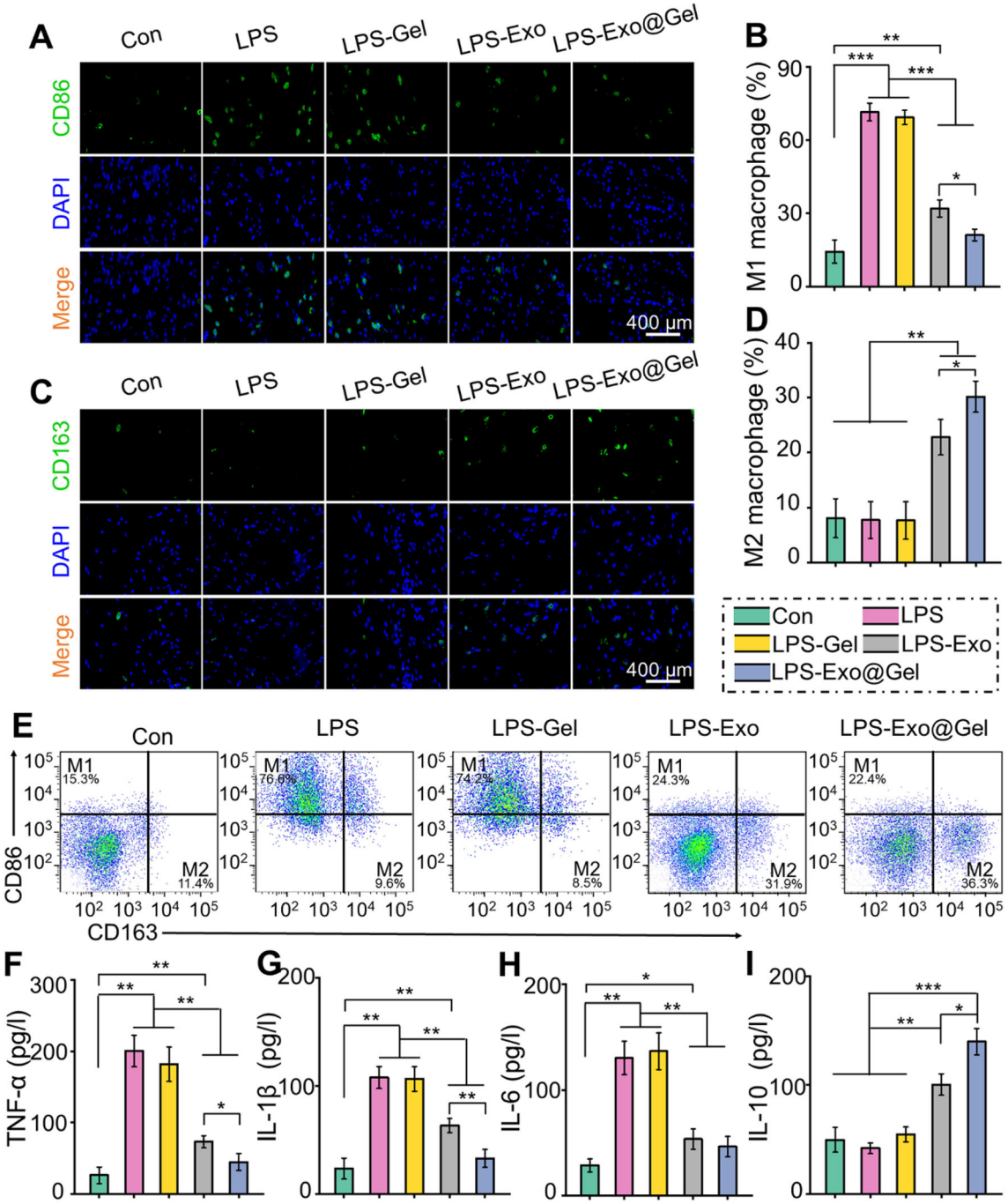

Fig. 5 Exo@Gel promotes the phenotypic transformation of macrophages from M1 to M2. **A**, **B** Immunofluorescence of CD86 (M1 marker) and statistical results. **C**, **D** Immunofluorescence of CD86 (M1 marker) and statistical results. **E** Representative flow cytometry plots show the expression of $CD86^{+}CD16^{3-}$ (M1) macrophages and $CD86^{-}CD163^{+}$ (M1) macrophages. **F–I** Evaluation of the cytokines, TNF-α, IL-1β, IL-6, and IL-10, in supernatants by ELISA (*$p < 0.05$, **$p < 0.01$, and ***$p < 0.001$)

time-consuming long period. Direct exosomes injection can partially affect the progression of OA, but it is difficult to durably retain exosomes at the damaged cartilage sites to exert their continuous chondroprotective effect. To prolong the bioactivity and actuation duration of exosomes in the articular cavity, the release profiles must be well controlled. In this study, we introduced a F127-HA hydrogel, in which exosomes could sustained release for up to 14 days. Histological observation demonstrated that this sustained-release strategy achieved a better result of preventing cartilage destruction than direct intra-articular injection of exosomes in OA.

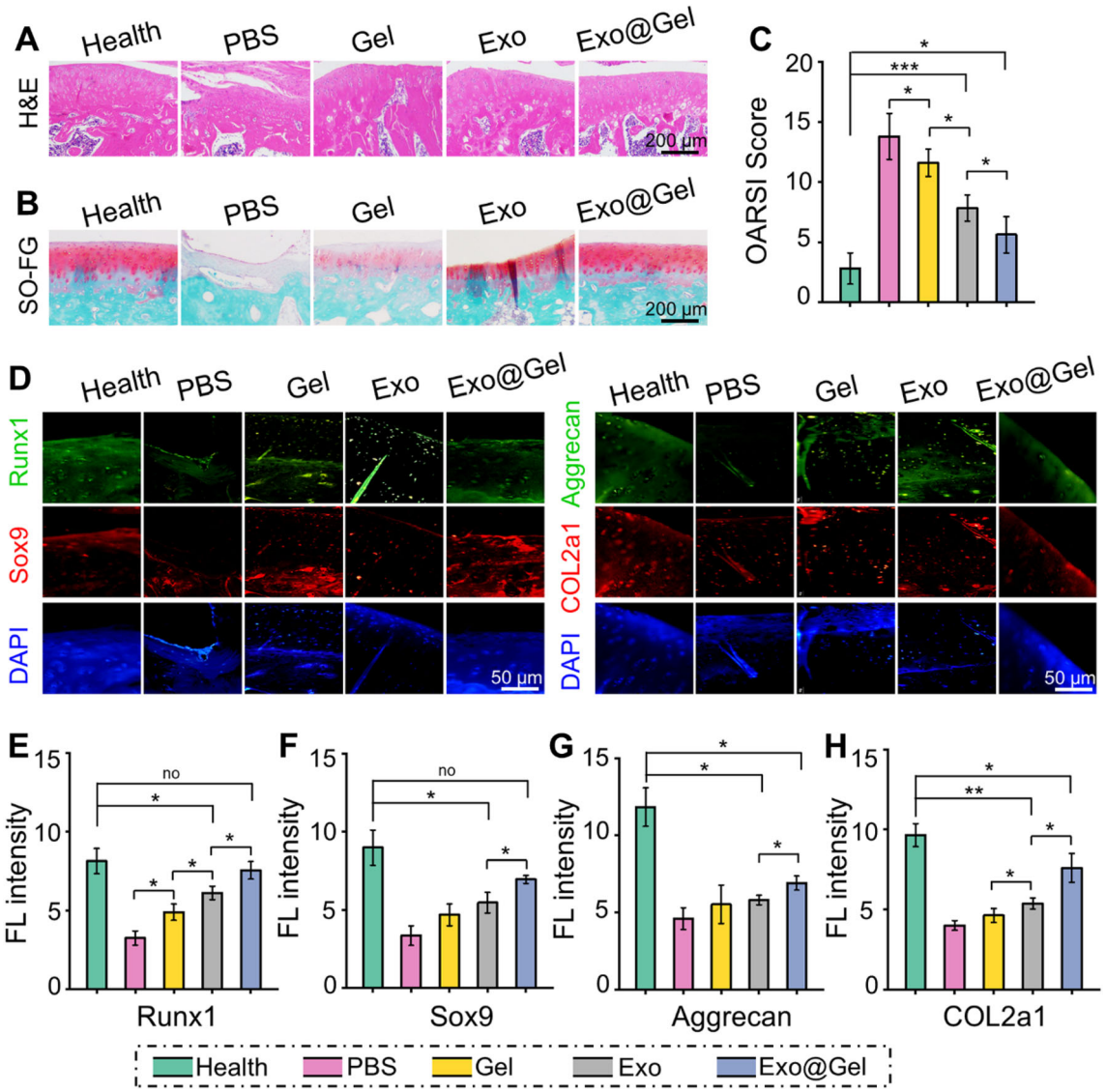

Fig. 6 Intra-articular injection of exosomes-incorporated F127-HA hydrogels reduce cartilage degeneration and enhance chondrogenesis in OA. **A** H&E staining of articular cartilage at 12 weeks after intra-articular injection. **B** Safranin O-fast green staining of articular cartilage at 12 weeks after intra-articular injection. **C** OARSI scores were statistically analyzed in each group. **D** Representative double immunofluorescence images of Runx1, Sox9, Aggrecan, and COL2a1 in cartilage at 12 weeks post-injection. **E–H** Quantitative analysis of fluorescence intensity Runx1, Sox9, Aggrecan, and COL2a1 in immunofluorescence staining ($*p < 0.05$, $**p < 0.01$, and $***p < 0.001$)

3.4.7 Intra-articular injection of Exo@Gel increases M2 macrophage polarization with a concomitant decrease in M1 macrophages and inflammatory cytokines

Studies have indicated that exosomes regulate macrophage polarization in many fields, thus, exhibiting an anti-inflammatory effect of immune regulation [15–20]. To study the mechanism of exosomes-incorporated hydrogel promoting articular cartilage repair, we investigated the polarization of macrophages in synovial tissue and cartilage, as well as the content of inflammatory cytokines in synovial fluid.

Synovial inflammation is associated with the pathogenesis of OA. Synovitis, which charactered by synovial tissue hyperplasia, inflammatory infiltration, and cell secretory dysfunction, is closely related to the polarization of synovial macrophages [51]. As shown in Fig. 7A, compared with the Health group, synovial hyperplasia and inflammatory cell infiltration were significantly increased in the PBS group. However, hydrogel, exosomes, and exosomes-incorporated hydrogel administration can partially alleviate the synovitis. Specifically, the

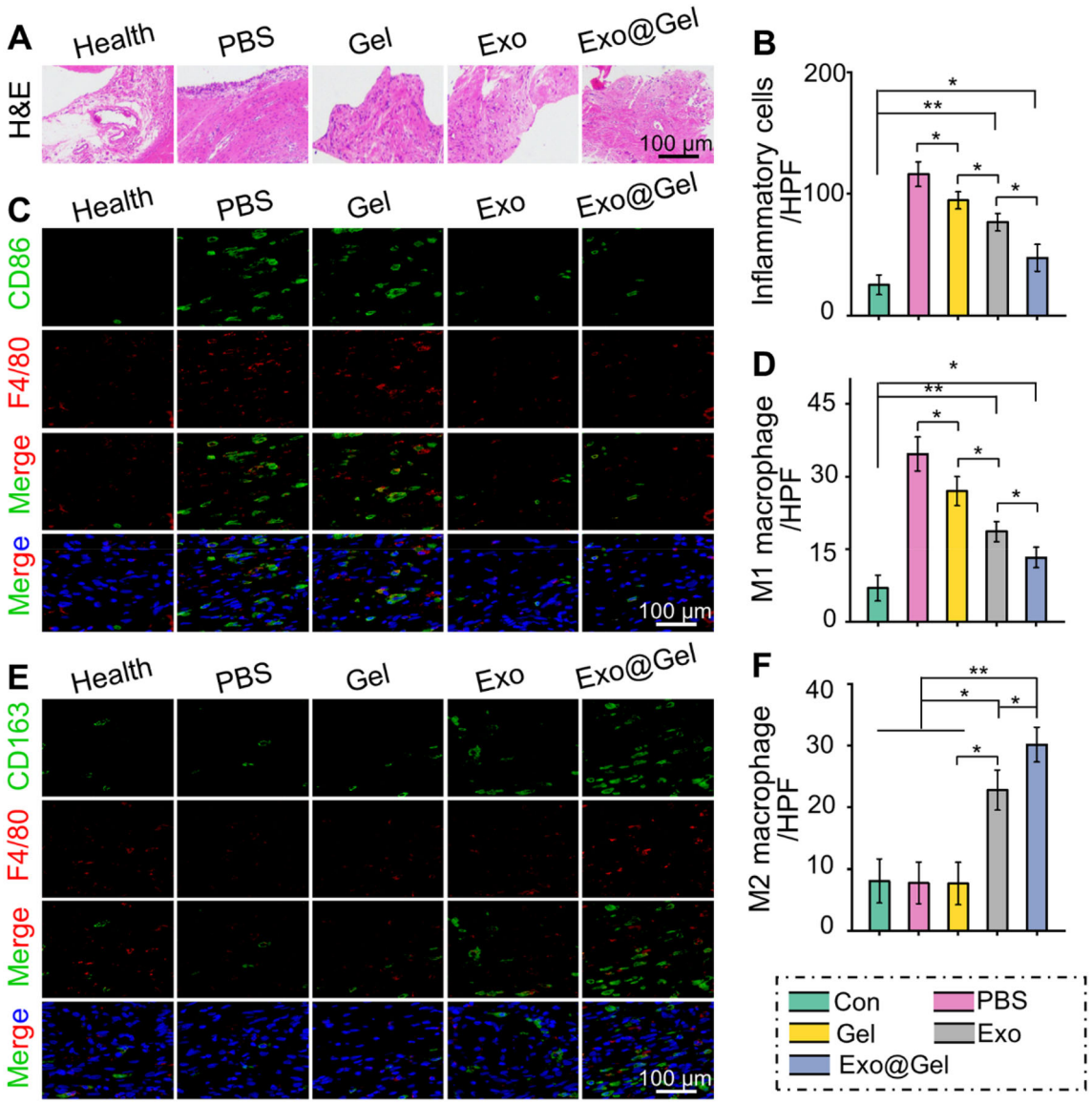

Fig. 7 Intra-articular injection of exosomes-incorporated F127-HA hydrogels promoted polarization of M1 to M2 macrophages in synovial tissue. **A** H&E staining of synovial tissue evaluate synovial inflammation. **B** Quantitative analysis of inflammatory cell infiltration in synovial tissue. **C**, **D** Immunohistochemical staining and quantitative analysis of F4/80 and CD86 positive cells (M1 macrophages) in synovial tissue. **E**, **F** Immunohistochemical staining and quantitative analysis of F4/80 and CD163 positive cells (M2 macrophages) in synovial tissue (*$p < 0.05$, **$p < 0.01$)

Exo@Gelgroup achieved the most significant effect on inhibiting inflammation deterioration among the OA models (Fig. 7B). As mentioned previously, M1 macrophages increase the inflammatory response during OA. Immunofluorescence images revealed that compared with Health group, the amount of F4/80 + CD86 positive cells (M1 macrophages) was significantly increased, while the proportion of F4/80 + CD163 positive cells (M2 macrophages) was not noticeably different in the PBS group and Gel group. However, the Exo@Gel group can greatly inhibit excessive M1 macrophage infiltration, while maximizing the formation of regenerative M2 macrophages in synovial tissue (Fig. 7C–F). In addition, in the cartilage tissue, Exo@Gel group also showed increased polarization of M2 macrophages, while reduced M1 macrophages infiltration (Fig. 8A–D).

It is well known that inflammatory response plays an important role in the pathogenesis of OA. During the pathological process of OA, pro-inflammatory cytokines and matrix metalloproteinases (MMP)-13 are rapidly up-regulated, accelerating chondrocyte apoptosis and matrix degradation. Previous studies have confirmed that excessive inflammatory reaction can aggravate OA severity by inducing cartilage degradation [52–54]. This excessive

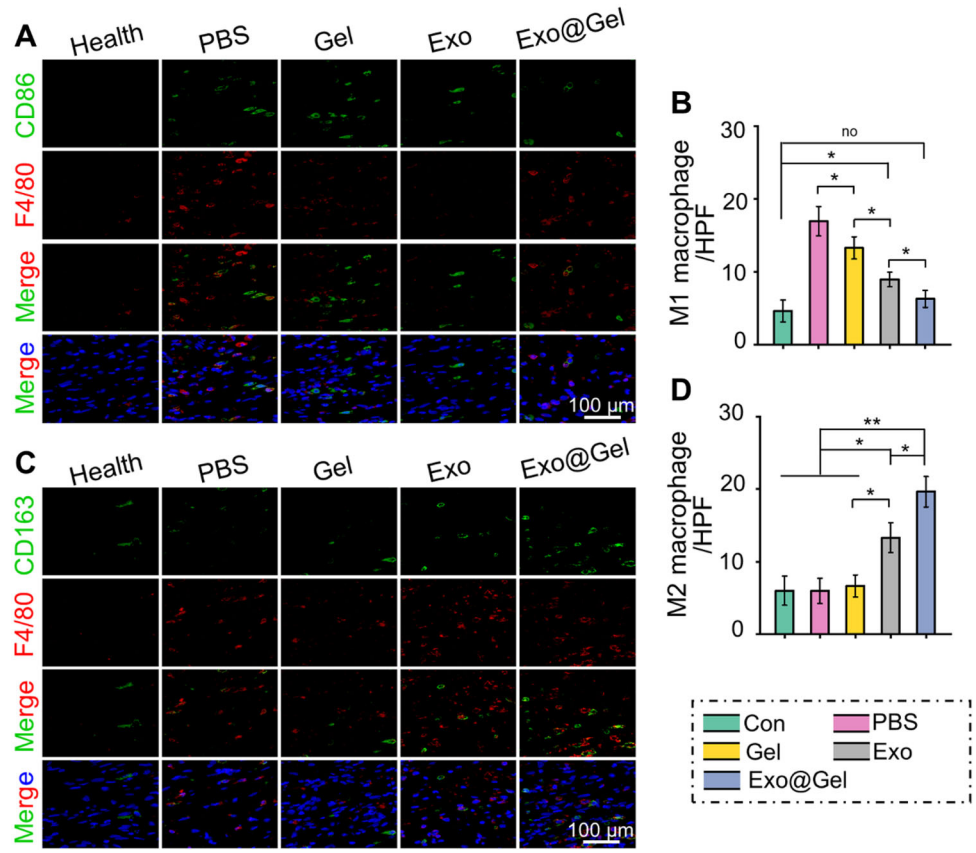

Fig. 8 Intra-articular injection of exosomes-incorporated F127-HA hydrogels promoted polarization of M1 to M2 macrophages in articular cartilage. **A**, **B** Immunohistochemical staining and quantitative analysis of F4/80 and CD86 positive cells (M1 macrophages) in articular cartilage. **C**, **D** Immunohistochemical staining and quantitative analysis of F4/80 and CD163 positive cells (M2 macrophages) in articular cartilage (*$p < 0.05$, **$p < 0.01$)

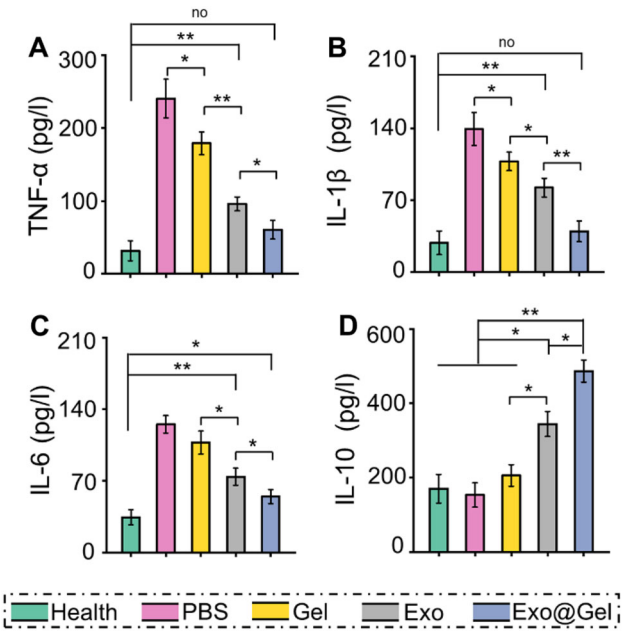

Fig. 9 Detection of inflammatory cytokines in synovial fluid. **A–C** The content of pro-inflammatory TNF-α, IL-1β, and IL-6 in synovial fluid. **D** The content of anti-inflammatory cytokine IL-10 in synovial fluid (*$p < 0.05$, **$p < 0.01$)

inflammation is associated with increased pro-inflammatory M1 macrophages and decreased regenerative M2 macrophages in OA tissues. For example, it has been reported that M1 macrophages in OA synovial tissue inhibit MSCs chondrogenic differentiation by secreting IL-6 [55]. Whereas M2 macrophages inhibit inflammation by secreting IL-10, which supports the survival of cartilage and improve OA symptoms [56, 57]. Therefore, we alleviate the inflammatory response by promoting macrophage polarization from M1 to M2, thereby alleviating the destruction of the cartilage matrix by excessive inflammation. ELISA detection of synovial fluid showed that the Exo@Gel group significantly decreased the levels of M1-associated pro-inflammatory cytokines TNF-α, IL-1β, and IL-6 (Fig. 9A–C), while increased the content of the anti-inflammatory cytokine IL-10 (Fig. 9D), which was consistent with the increased polarization of M2 macrophages and concomitant decrease in M1 macrophages. These findings indicated that exosomes-incorporated hydrogel promoted the polarization of M1 to M2 macrophages in synovial tissue and cartilage during OA progression, decreased the pro-inflammatory cytokines and increased the anti-inflammatory cytokines in synovial fluid, thus preventing articular cartilage destruction in OA.

In conclusion, a novel intra-articular strategy, namely, incorporating the primary chondrocyte-derived exosomes into thermosensitive hydrogel, was designed for the treatment of OA. Sustained release of exosomes from the hydrogel can promote chondrocytes proliferation, migration, and matrix synthesis. Significantly, intra-articular injection of this exosomes-incorporated hydrogel provided with efficient outcome of preventing cartilage destruction by promoting polarization of M1 to M2 macrophages and reducing excessive inflammation in the articular microenvironment, suggesting a great prospect in the treatment of OA.

Acknowledgements This research was financially supported by the National Natural Science Foundation of China (82072533), the Science and Technology Committee of Fengxian District, Shanghai (20201501).

Declaration

Conflict of interest All authors declare no conflict of interest.

Ethical statement All animal procedures were performed in accordance with the guidelines for Care and Use of Laboratory Animal Experience and approved by the Animal Care and Use Ethics Committee of Northern Jiangsu People's Hospital (IACUC no. 20170312001).

References

1. Peat G, Thomas MJ. Osteoarthritis year in review 2020: epidemiology & therapy. Osteoarthritis Cartilage. 2021;29:180–9.
2. Huey DJ, Hu JC, Athanasiou KA. Unlike bone, cartilage regeneration remains elusive. Science. 2012;338:917–21.
3. Bai H, Zhao Y, Wang C, Wang Z, Wang J, Liu H, et al. Enhanced osseointegration of three-dimensional supramolecular bioactive interface through osteoporotic microenvironment regulation. Theranostics. 2020;10:4779–94.
4. Zhao Y, Li Z, Jiang Y, Liu H, Feng Y, Wang Z, et al. Bioinspired mineral hydrogels as nanocomposite scaffolds for the promotion of osteogenic marker expression and the induction of bone regeneration in osteoporosis. Acta Biomater. 2020;113:614–26.
5. Yu W, Hu B, Boakye-Yiadom KO, Ho W, Chen Q, Xu X, et al. Injectable hydrogel mediated delivery of gene-engineered adipose-derived stem cells for enhanced osteoarthritis treatment. Biomaterials Science. 2021;9:7603–16.
6. Nguyen TH, Duong CM, Nguyen XH, Than UTT. Mesenchymal stem cell-derived extracellular vesicles for osteoarthritis treatment: extracellular matrix protection, chondrocyte and osteocyte physiology, pain and inflammation management. Cells. 2021;10:2887.
7. Sanghani-Kerai A, Black C, Cheng SO, Collins L, Schneider N, Blunn G, et al. Clinical outcomes following intra-articular injection of autologous adipose-derived mesenchymal stem cells for the treatment of osteoarthritis in dogs characterized by weight-bearing asymmetry. Bone Joint Res. 2021;10:650–8.
8. Chen CF, Hu CC, Wu CT, Wu HH, Chang CS, Hung YP, et al. Treatment of knee osteoarthritis with intra-articular injection of allogeneic adipose-derived stem cells (ADSCs) ELIXCYTE ®: a phase I/II, randomized, active-control, single-blind, multiple-center clinical trial. Stem Cell Res Ther. 2021;12:562.
9. Liu X, Yang Y, Li Y, Niu X, Zhao B, Wang Y, et al. Integration of stem cell-derived exosomes with in situ hydrogel glue as a promising tissue patch for articular cartilage regeneration. Nanoscale. 2017;9:4430–8.
10. Chang YH, Liu HW, Wu KC, Ding DC. Mesenchymal stem cells and their clinical applications in osteoarthritis. Cell Transplant. 2016;25:937–50.
11. Ha CW, Park YB, Kim SH, Lee HJ. Intra-articular mesenchymal stem cells in osteoarthritis of the knee: a systematic review of clinical outcomes and evidence of cartilage repair. Arthroscopy. 2019;35:277–88.e2.
12. Savkovic V, Li H, Seon JK, Hacker M, Franz S, Simon JC. Mesenchymal stem cells in cartilage regeneration. Curr Stem Cell Res Ther. 2014;9:469–88.
13. Doyle EC, Wragg NM, Wilson SL. Intraarticular injection of bone marrow-derived mesenchymal stem cells enhancesregeneration in knee osteoarthritis. Knee Surg Sports Traumatol Arthrosc. 2020;28:3827–42.
14. Lee Y, Park YS, Choi NY, Kim YI, Koh YG. Proteomic analysis reveals commonly secreted proteins of mesenchymal stem cells derived from bone marrow, adipose tissue, and synovial membrane to show potential for cartilage regeneration in knee osteoarthritis. Stem Cells Int. 2021;2021:6694299.
15. Zhang J, Rong Y, Luo C, Cui W. Bone marrow mesenchymal stem cell-derived exosomes prevent osteoarthritis by regulating synovial macrophage polarization. Aging (Albany NY). 2020;12:25138–52.
16. Mianehsaz E, Mirzaei HR, Mahjoubin-Tehran M, Rezaee A, Sahebnasagh R, Pourhanifeh MH, et al. Mesenchymal stem cell-derived exosomes: a new therapeutic approach to osteoarthritis? Stem Cell Res Ther. 2019;10:340.
17. Lee JC, Choe SY. Gene alterations after human adipose-derived stem cell-derived exosome injection in monosodium iodoacetate-induced osteoarthritis rats by microarray analysis. J Anat Soc India. 2020;69:37–47.
18. Wang Y, Yu D, Liu Z, Zhou F, Dai J, Wu B, et al. Exosomes from embryonic mesenchymal stem cells alleviate osteoarthritis through balancing synthesis and degradation of cartilage extracellular matrix. Stem Cell Res Ther. 2017;8:189.
19. Tao SC, Yuan T, Zhang YL, Yin WJ, Guo SC, Zhang CQ. Exosomes derived from miR-140-5p-overexpressing human synovial mesenchymal stem cells enhance cartilage tissue regeneration and prevent osteoarthritis of the knee in a rat model. Theranostics. 2017;7:180–95.
20. Zheng L, Wang Y, Qiu P, Xia C, Fang Y, Mei S, et al. Primary chondrocyte exosomes mediate osteoarthritis progression by regulating mitochondrion and immune reactivity. Nanomedicine (Lond). 2019;14:3193–212.
21. Nikhil A, Kumar A. Evaluating potential of tissue-engineered cryogels and chondrocyte derived exosomes in articular cartilage repair. Biotechnol Bioeng. 2022;119:605–25.
22. Patel JM, Loebel C, Saleh KS, Wise BC, Bonnevie ED, Miller LM, et al. Stabilization of damaged articular cartilage with hydrogel-mediated reinforcement and sealing. Adv Healthc Mater. 2021;10:e2100315.
23. Antich C, Jiménez G, de Vicente J, López-Ruiz E, Chocarro-Wrona C, Griñán-Lisón C, et al. Development of a biomimetic hydrogel based on predifferentiated mesenchymal stem-cell-derived ECM for cartilage tissue engineering. Adv Healthc Mater. 2021;10:e2001847.
24. Zhao Y, Li Z, Song S, Yang K, Liu H, Yang Z, et al. Skin-inspired antibacterial conductive hydrogels for epidermal sensors and diabetic foot wound dressings. Adv Funct Mater. 2019;29:1901474.
25. Li Z, Zhao Y, Liu H, Ren M, Wang Z, Wang X, et al. pH-responsive hydrogel loaded with insulin as a bioactive dressing

for enhancing diabetic wound healing. Mate Des. 2021; 210:110104.
26. Bai H, Kyu-Cheol N, Wang Z, Cui Y, Liu H, Liu H, et al. Regulation of inflammatory microenvironment using a self-healing hydrogel loaded with BM-MSCs for advanced wound healing in rat diabetic foot ulcers. J Tissue Eng. 2020;11:2041731420947242.
27. Gosset M, Berenbaum F, Thirion S, Jacques C. Primary culture and phenotyping of murine chondrocytes. Nat Protoc. 2008;3:1253–60.
28. Wang K, Dong R, Tang J, Li H, Dang J, Zhang Z, et al. Exosomes laden self-healing injectable hydrogel enhances diabetic wound healing via regulating macrophage polarization to accelerate angiogenesis. Chem Eng J. 2022; 430;132664.
29. Jung YS, Park W, Park H, Lee DK, Na K. Thermo-sensitive injectable hydrogel based on the physical mixing of hyaluronic acid and Pluronic F-127 for sustained NSAID delivery. Carbohydr Polym. 2017;156:403–8.
30. Hsieh HY, Lin WY, Lee AL, Li YC, Chen YJ, Chen KC, et al. Hyaluronic acid on the urokinase sustained release with a hydrogel system composed of poloxamer 407: HA/P407 hydrogel system for drug delivery. Plos One. 2020;15:e0227784.
31. Kang ML, Jeong SY, Im GI. Hyaluronic acid hydrogel functionalized with self-assembled micelles of amphiphilic PEGylated kartogenin for the treatment of osteoarthritis. Tissue Eng Part A. 2017;23:630–9.
32. Bai H, Cui Y, Wang C, Wang Z, Luo W, Liu Y, et al. 3D printed porous biomimetic composition sustained release zoledronate to promote osteointegration of osteoporotic defects. Mater Des. 2020;189:108513.
33. Yang HM, Yoon HY, Kim CH, Goo YT, Choi IJ, Park SG, et al. Poloxamer 407-based floating hydrogels for intravesical instillation: statistical optimization using central composite design, gel erosion, and drug release. Bull Korean Chem Soc. 2021;42:72–9.
34. Tundisi LL, Yang R, Borelli LPP, Alves T, Mehta M, Chaud MV, Mazzola PG, Kohane DS. Enhancement of the mechanical and drug-releasing properties of Poloxamer 407 hydrogels with casein. Pharm Res. 2021;38:515–22.
35. He Z, Wang B, Hu C, Zhao J. An overview of hydrogel-based intra-articular drug delivery for the treatment of osteoarthritis. Colloids Surf B Biointerfaces. 2017;154:33–9.
36. Henrotin Y, Raman R, Richette P, Bard H, Jerosch J, Conrozier T, et al. Consensus statement on viscosupplementation with hyaluronic acid for the management of osteoarthritis. Semin Arthritis Rheum. 2015;45:140–9.
37. Yano F, Ohba S, Murahashi Y, Tanaka S, Saito T, Chung UI. Runx1 contributes to articular cartilage maintenance by enhancement of cartilage matrix production and suppression of hypertrophic differentiation. Sci Rep. 2019;9:7666.
38. Lefebvre V, Angelozzi M, Haseeb A. SOX9 in cartilage development and disease. Curr Opin Cell Biol. 2019;61:39–47.
39. Haseeb A, Kc R, Angelozzi M, de Charleroy C, Rux D, Tower RJ, et al. SOX9 keeps growth plates and articular cartilage healthy by inhibiting chondrocyte dedifferentiation/osteoblastic redifferentiation. Proc National Acad Sci U S A. 2021;118:e2019152118.
40. Xu X, Liang Y, Li X, Ouyang K, Wang M, Cao T, et al. Exosome-mediated delivery of kartogenin for chondrogenesis of synovial fluid-derived mesenchymal stem cells and cartilage regeneration. Biomaterials. 2021;269:120539.
41. Lee GW, Thangavelu M, Choi MJ, Shin EY, Kim HS, Baek JS, et al. Exosome mediated transfer of miRNA-140 promotes enhanced chondrogenic differentiation of bone marrow stem cells for enhanced cartilage repair and regeneration. J Cell Biochem. 2020;121:3642–52.
42. Zhang S, Chuah SJ, Lai RC, Hui JHP, Lim SK, Toh WS. MSC exosomes mediate cartilage repair by enhancing proliferation, attenuating apoptosis and modulating immune reactivity. Biomaterials. 2018;156:16–27.
43. Su N, Hao Y, Wang F, Hou W, Chen H, Luo Y. Mesenchymal stromal exosome-functionalized scaffolds induce innate and adaptive immunomodulatory responses toward tissue repair. Sci Adv. 2021;7:eabf7207.
44. He Y, Tian M, Li X, Hou J, Chen S, Yang G, et al. A hierarchical-structured mineralized nanofiber scaffold with osteoimmunomodulatory and osteoinductive functions for enhanced alveolar bone regeneration. Adv Healthc Mater. 2022;11:e2102236.
45. Li X, Wang X, Liu Q, Yan J, Pan D, Wang L, et al. ROS-responsive boronate-stabilized polyphenol-poloxamer 188 assembled dexamethasone nanodrug for macrophage repolarization in osteoarthritis treatment. Adv Healthc Mater. 2021;10:e2100883.
46. Youn YJ, Shrestha S, Lee YB, Kim JK, Lee JH, Hur K, et al. Neutrophil-derived trail is a proinflammatory subtype of neutrophil-derived extracellular vesicles. Theranostics. 2021;11:2770–87.
47. Camarero-Espinosa S, Carlos-Oliveira M, Liu H, Mano JF, Bouvy N, Moroni L. 3D Printed dual-porosity scaffolds: the combined effect of stiffness and porosity in the modulation of macrophage polarization. Adv Healthc Mater. 2022;11:e2101415.
48. Bai JY, Li Y, Xue GH, Li KR, Zheng YF, Zhang ZQ, et al. Requirement of G alpha i1 and G alpha i3 in interleukin-4-induced signaling, macrophage M2 polarization and allergic asthma response. Theranostics. 2021;11:4894–909.
49. Mao G, Xu Y, Long D, Sun H, Li H, Xin R, et al. Exosome-transported circRNA_0001236 enhances chondrogenesis and suppress cartilage degradation via the miR-3677–3p/Sox9 axis. Stem Cell Res Ther. 2021;12:389.
50. Duan L, Xu X, Xu L, Chen H, Li X, Alahdal M, et al. Exosome-mediated drug delivery for cell-free therapy of osteoarthritis. Curr Med Chem. 2021;28:6458–83.
51. Atukorala I, Kwoh CK, Guermazi A, Roemer FW, Boudreau RM, Hannon MJ, et al. Synovitis in knee osteoarthritis: a precursor of disease? Ann Rheum Dis. 2016;75:390–5.
52. Kwon JY, Lee SH, Na HS, Jung K, Choi J, Cho KH, et al. Kartogenin inhibits pain behavior, chondrocyte inflammation, and attenuates osteoarthritis progression in mice through induction of IL-10. Sci Rep. 2018;8:13832.
53. Hu QC, Ecker M. Overview of MMP-13 as a promising target for the treatment of osteoarthritis. Int J Mol Sci. 2021;22:1742.
54. Lan QM, Lu RB, Chen HM, Pang YF, Xiong F, Shen C, et al. MMP-13 enzyme and pH responsive theranostic nanoplatform for osteoarthritis. J Nanobiotechnology. 2020;18:117.
55. Fahy N, de Vries-van Melle ML, Lehmann J, Wei W, Grotenhuis N, Farrell E, et al. Human osteoarthritic synovium impacts chondrogenic differentiation of mesenchymal stem cells via macrophage polarisation state. Osteoarthritis Cartilage. 2014;22:1167–75.
56. Kwon JY, Lee SH, Na HS, Jung K, Choi J, Cho KH, et al. Kartogenin inhibits pain behavior, chondrocyte inflammation, and attenuates osteoarthritis progression in mice through induction of IL-10. Sci Rep. 2018;8:13832.
57. Ding J, Chen B, Lv T, Liu X, Fu X, Wang Q, et al. Bone marrow mesenchymal stem cell-based engineered cartilage ameliorates polyglycolic acid/polylactic acid scaffold-induced inflammation through M2 polarization of macrophages in a pig model. Stem Cells Transl Med. 2016;5:1079–89.